First CLAS12 Measurement of Deeply Virtual Compton Scattering Beam-Spin Asymmetries in the Extended Valence Region

G. Christiaens,[1,2] M. Defurne,[1,*] D. Sokhan,[1,2] P. Achenbach,[3] Z. Akbar,[4] M. J. Amaryan,[5] H. Atac,[6] H. Avakian,[3] C. Ayerbe Gayoso,[7] L. Baashen,[8] N. A. Baltzell,[3] L. Barion,[9] M. Bashkanov,[10] M. Battaglieri,[11] I. Bedlinskiy,[12] B. Benkel,[13] F. Benmokhtar,[14] A. Bianconi,[15,16] A. S. Biselli,[17] M. Bondi,[18] W. A. Booth,[10] F. Bossù,[1] S. Boiarinov,[3] K.-Th. Brinkmann,[19] W. J. Briscoe,[20] S. Bueltmann,[5] D. Bulumulla,[5] V. D. Burkert,[3] T. Cao,[3] D. S. Carman,[3] J. C. Carvajal,[8] A. Celentano,[11] P. Chatagnon,[21] V. Chesnokov,[22] T. Chetry,[8,23,24] G. Ciullo,[9,25] G. Clash,[10] P. L. Cole,[26,27,3] M. Contalbrigo,[9] G. Costantini,[15,16] A. D'Angelo,[18,28] N. Dashyan,[29] R. De Vita,[11] A. Deur,[3] S. Diehl,[19,30] C. Dilks,[31] C. Djalali,[24,32] R. Dupre,[21] H. Egiyan,[3] M. Ehrhart,[21,†] A. El Alaoui,[13] L. El Fassi,[23] L. Elouadrhiri,[3] S. Fegan,[10] A. Filippi,[33] K. Gates,[2] G. Gavalian,[3] Y. Ghandilyan,[29] G. P. Gilfoyle,[34] F. X. Girod,[3] D. I. Glazier,[2] A. A. Golubenko,[22] G. Gosta,[15] R. W. Gothe,[32] Y. Gotra,[3] K. A. Griffioen,[7] M. Guidal,[21] K. Hafidi,[35] H. Hakobyan,[13] M. Hattawy,[5,35] F. Hauenstein,[3,5] T. B. Hayward,[30] D. Heddle,[36,3] A. Hobart,[21] D. E. Holmberg,[7] M. Holtrop,[37] Y. Ilieva,[32] D. G. Ireland,[2] E. L. Isupov,[22] H. S. Jo,[38] D. Keller,[4] M. Khachatryan,[5] A. Khanal,[8] W. Kim,[38] A. Kripko,[19] V. Kubarovsky,[3] S. E. Kuhn,[5] V. Lagerquist,[5] L. Lanza,[18] M. L. Kabir,[23] M. Leali,[15,16] S. Lee,[39,†] P. Lenisa,[9,25] X. Li,[39] K. Livingston,[2] I. J. D. MacGregor,[2] D. Marchand,[21] V. Mascagna,[15,40,16] G. Matousek,[31] B. McKinnon,[2] C. McLauchlin,[32] Z. E. Meziani,[35,6] S. Migliorati,[15,16] R. G. Milner,[39] T. Mineeva,[13] M. Mirazita,[41] V. Mokeev,[3] E. Molina,[13] C. Munoz Camacho,[21] P. Nadel-Turonski,[3] P. Naidoo,[2] K. Neupane,[32] S. Niccolai,[21] M. Nicol,[10] G. Niculescu,[42] M. Osipenko,[11] M. Ouillon,[21] P. Pandey,[5] M. Paolone,[43,6] L. L. Pappalardo,[9,25] R. Paremuzyan,[3,37] E. Pasyuk,[3] S. J. Paul,[44] W. Phelps,[36,20] N. Pilleux,[21] M. Pokhrel,[5] J. Poudel,[5] J. W. Price,[45] Y. Prok,[5] A. Radic,[13] N. Ramasubramanian,[1] B. A. Raue,[8] Trevor Reed,[8] J. Richards,[30] M. Ripani,[11] J. Ritman,[46,47] P. Rossi,[3,41] F. Sabatié,[1] C. Salgado,[48] S. Schadmand,[46,47] A. Schmidt,[20,39] M. B. C. Scott,[35] Y. G. Sharabian,[3] E. V. Shirokov,[22] U. Shrestha,[30,24] P. Simmerling,[30] N. Sparveris,[6] M. Spreafico,[11] S. Stepanyan,[3] I. I. Strakovsky,[20] S. Strauch,[32] J. A. Tan,[38] N. Trotta,[30] M. Turisini,[41] R. Tyson,[2] M. Ungaro,[3] S. Vallarino,[9] L. Venturelli,[15,16] H. Voskanyan,[29] E. Voutier,[21] D. P. Watts,[10] X. Wei,[3] R. Williams,[10] R. Wishart,[2] M. H. Wood,[49] N. Zachariou,[10] J. Zhang,[4] Z. W. Zhao,[31,5] V. Ziegler,[3] and M. Zurek[35]

(CLAS Collaboration)

[1]*IRFU, CEA, Université Paris-Saclay, F-91191 Gif-sur-Yvette, France*
[2]*University of Glasgow, Glasgow G12 8QQ, United Kingdom*
[3]*Thomas Jefferson National Accelerator Facility, Newport News, Virginia 23606, USA*
[4]*University of Virginia, Charlottesville, Virginia 22901, USA*
[5]*Old Dominion University, Norfolk, Virginia 23529, USA*
[6]*Temple University, Philadelphia, Pennsylvania 19122, USA*
[7]*College of William and Mary, Williamsburg, Virginia 23187-8795, USA*
[8]*Florida International University, Miami, Florida 33199, USA*
[9]*INFN, Sezione di Ferrara, 44100 Ferrara, Italy*
[10]*University of York, York YO10 5DD, United Kingdom*
[11]*INFN, Sezione di Genova, 16146 Genova, Italy*
[12]*National Research Centre Kurchatov Institute—ITEP, Moscow, 117259, Russia*
[13]*Universidad Técnica Federico Santa María, Casilla 110-V Valparaíso, Chile*
[14]*Duquesne University, 600 Forbes Avenue, Pittsburgh, Pennsylvania 15282, USA*
[15]*Universit'a degli Studi di Brescia, 25123 Brescia, Italy*
[16]*INFN, Sezione di Pavia, 27100 Pavia, Italy*
[17]*Fairfield University, Fairfield, Connecticut 06824, USA*
[18]*INFN, Sezione di Roma Tor Vergata, 00133 Rome, Italy*
[19]*II Physikalisches Institut der Universitaet Giessen, 35392 Giessen, Germany*
[20]*The George Washington University, Washington, D.C. 20052, USA*
[21]*Université Paris-Saclay, CNRS/IN2P3, IJCLab, 91405 Orsay, France*
[22]*Skobeltsyn Institute of Nuclear Physics, Lomonosov Moscow State University, 119234 Moscow, Russia*
[23]*Mississippi State University, Mississippi State, Mississippi 39762-5167, USA*
[24]*Ohio University, Athens, Ohio 45701, USA*
[25]*Universita' di Ferrara, 44121 Ferrara, Italy*

[26]Lamar University, 4400 MLK Boulevard, P.O. Box 10046, Beaumont, Texas 77710, USA
[27]Catholic University of America, Washington, D.C. 20064, USA
[28]Universita' di Roma Tor Vergata, 00133 Rome, Italy
[29]Yerevan Physics Institute, 375036 Yerevan, Armenia
[30]University of Connecticut, Storrs, Connecticut 06269, USA
[31]Duke University, Durham, North Carolina 27708-0305, USA
[32]University of South Carolina, Columbia, South Carolina 29208, USA
[33]INFN, Sezione di Torino, 10125 Torino, Italy
[34]University of Richmond, Richmond, Virginia 23173, USA
[35]Argonne National Laboratory, Argonne, Illinois 60439, USA
[36]Christopher Newport University, Newport News, Virginia 23606, USA
[37]University of New Hampshire, Durham, New Hampshire 03824-3568, USA
[38]Kyungpook National University, Daegu 41566, Republic of Korea
[39]Massachusetts Institute of Technology, Cambridge, Massachusetts 02139-4307, USA
[40]Università degli Studi dell'Insubria, 22100 Como, Italy
[41]INFN, Laboratori Nazionali di Frascati, 00044 Frascati, Italy
[42]James Madison University, Harrisonburg, Virginia 22807, USA
[43]New Mexico State University, P.O. Box 30001, Las Cruces, New Mexico 88003, USA
[44]University of California Riverside, 900 University Avenue, Riverside, California 92521, USA
[45]California State University, Dominguez Hills, Carson, California 90747, USA
[46]GSI Helmholtzzentrum fur Schwerionenforschung GmbH, D 64291 Darmstadt, Germany
[47]Institute fur Kernphysik (Juelich), 52428 Juelich, Germany
[48]Norfolk State University, Norfolk, Virginia 23504, USA
[49]Canisius College, Buffalo, New York 14208, USA

(Received 5 December 2022; revised 24 March 2023; accepted 21 April 2023; published 25 May 2023)

Deeply virtual Compton scattering (DVCS) allows one to probe generalized parton distributions describing the 3D structure of the nucleon. We report the first measurement of the DVCS beam-spin asymmetry using the CLAS12 spectrometer with a 10.2 and 10.6 GeV electron beam scattering from unpolarized protons. The results greatly extend the Q^2 and Bjorken-x phase space beyond the existing data in the valence region and provide 1600 new data points measured with unprecedented statistical uncertainty, setting new, tight constraints for future phenomenological studies.

DOI: 10.1103/PhysRevLett.130.211902

Introduction.—Generalized parton distributions (GPDs) serve as a powerful tool for describing the three-dimensional dynamics of nucleon structure, including the composition of spin and pressure distributions [1–5]. These functions can be accessed via exclusive processes in deep inelastic scattering, where the squared four-momentum transfer from the lepton to a parton in the nucleon is quantified by Q^2 and the resulting change in the nucleon's momentum is contained in the Mandelstam variable t.

Deeply virtual Compton scattering (DVCS) is characterized by the struck parton (with longitudinal momentum fraction x) emitting a high-energy photon and the nucleon remaining intact (Fig. 1). The amplitudes of the process are parametrized by Compton form factors (CFFs), complex functions that are x integrals of the corresponding GPDs. DVCS is sensitive, at high Q^2, low t, and leading order in perturbative quantum chromodynamics, to the CFFs corresponding to four GPDs: H, E, $\tilde{H}$, and $\tilde{E}$ [1–4]. In the experimentally indistinguishable process, Bethe-Heitler (BH) process, the photon is instead radiated by the incoming or scattered lepton. As BH and DVCS share the same final state, the observed photon electroproduction

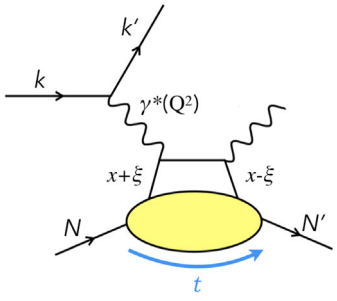

FIG. 1. DVCS: an electron of momentum k scatters from a parton in a nucleon of momentum N. As a result, there is a change of 2ξ in the parton's longitudinal momentum fraction.

Published by the American Physical Society under the terms of the Creative Commons Attribution 4.0 International license. Further distribution of this work must maintain attribution to the author(s) and the published article's title, journal citation, and DOI. Funded by SCOAP³.

results from the interference of both processes and the cross section can be written as

$$\sigma^{e^{\pm}p\gamma} = \sigma^{\mathrm{BH}} + \sigma^{\mathrm{DVCS}} \mp (\mathcal{I}^{\mathrm{Re}} + \lambda_e \mathcal{I}^{\mathrm{Im}}), \qquad (1)$$

where λ_e is the beam polarization, σ^{BH} and σ^{DVCS} are the cross sections of BH and DVCS, respectively, and $\mathcal{I}^{\mathrm{Re}}$ and $\mathcal{I}^{\mathrm{Im}}$ are the real and imaginary parts of the interference term between the amplitudes for both processes.

The beam-spin asymmetry in photon electroproduction is an experimentally attractive observable, since, to first approximation, detector acceptance effects cancel. Produced mostly by the interference of BH and DVCS, for a proton target in the valence region, it can reach up to ∼20% (as observed in the previously collected data) and is dominated by Im$\mathcal{H}$, the imaginary part of the CFF corresponding to the GPD H [6,7].

Exclusive photon electroproduction on the nucleon has been successfully studied at a number of facilities around the world, such as DESY with H1 [8–11], ZEUS [12,13], HERMES [14], COMPASS [15,16], and Jefferson Lab Halls A [17–22] and B [23–29]. In this Letter, we report the first DVCS measurements performed with a beam energy of just over 10 GeV and the CLAS12 spectrometer in Hall B at Jefferson Lab. Approximately 89% of the new data cover a phase space in the valence quark region that has never been probed with DVCS before. The data were collected in the fall of 2018 with a beam energy of 10.6 GeV and in the spring of 2019 at 10.2 GeV. For both run periods, which used an unpolarized liquid-H_2 target, the longitudinal beam polarization was ∼86%. This, along with very large statistics, enabled measurements of the beam-spin asymmetry in DVCS off the proton to be made in 64 bins of x_B, Q^2, and t.

The CLAS12 spectrometer.—The CLAS12 spectrometer [30] can be decomposed into a central and a forward part. The central part, around the target, is placed in a 5 T solenoidal magnetic field, detecting particles emitted at polar angles between 35° and 125° with respect to the beam direction. Silicon and Micromegas trackers are used to reconstruct charged tracks, while a time-of-flight scintillator detector enables particle identification. At the heart of the forward part are drift chambers placed in a toroidal magnetic field for charged track reconstruction. Electron identification is provided by a high-threshold Čerenkov detector complemented with an electromagnetic sampling calorimeter. Hadrons are identified using a scintillator time-of-flight detector placed between the drift chambers and the calorimeter.

Scattered electrons are detected in the forward part of CLAS12. About 80% of the recoil protons are detected in the central part, while the remaining 20% go forward. Finally, the photon is detected either in the electromagnetic calorimeter or in a specialized forward tagger, designed to cover polar angles of 2°–5° from the beam direction.

Beam-spin asymmetry in $ep \to e'p'\gamma$.—Events with a single high-energy electron, a single proton, and at least one photon above 2 GeV were considered as BH-DVCS candidates. The highest-energy photon is selected if more than one meets the criteria in the event. Exclusivity was ensured by application of cuts on the following variables:

$\theta_{\gamma\gamma}$: The cone angle between the detected photon and the expected photon direction in $ep \to e'p'\gamma$, derived kinematically using the scattered electron, the detected proton, and momentum conservation. It is cut at 0.6° and shown in Fig. 2 (right).

E_{miss}: The "missing" energy balance between the initial state, ep, and the $e'p'\gamma$ final state. It is cut at 0.5 GeV.

$p_{T\mathrm{miss}}$: The missing transverse (with respect to the beam) momentum balance between the ep and the $e'p'\gamma$ states is cut at 0.125 MeV.

$M^2_{e'\gamma X}$: The squared missing mass of X in the process $ep \to e'\gamma X$, which should correspond to a proton for exclusive reconstruction of DVCS or BH and is consequently cut at 1.25 GeV^2. The distribution is displayed in Fig. 2 (left).

The main background to the DVCS-BH process, which is reduced but not entirely eliminated by the exclusivity cuts, comes from π^0 electroproduction. In this process, instead of a photon, the target proton emits a neutral pion with energy similar to that of a DVCS photon, since the pion mass is low. The exclusive π^0 production is also sensitive to GPDs and carries its own beam-spin asymmetry, although it is typically on the few-percent level [31] and much lower than that of DVCS-BH.

In its center-of-mass frame, the pion decays into two back-to-back photons, but in the laboratory frame, their direction and energy depend on the relative orientation of their momenta with respect to the boost direction defined by the pion momentum. When the decay is collinear to the pion momentum, one photon carries almost all of the pion energy and may mimic a DVCS photon, passing the exclusivity cuts. To subtract this contamination, we applied the technique developed in [18]. Applying identical selection criteria for the electron and the proton as in the DVCS analysis, a π^0 sample was created from the data by cutting on the two-photon invariant mass and loosely cutting on $M^2_{e'\gamma\gamma X}$, the squared missing mass associated with X in $ep \to e'\gamma\gamma X$. This selects a sample of $ep \to e'p'\pi^0$ events. Next, for each π^0 in this sample, the associated DVCS contamination was derived by generating 1500 decays of $\pi^0 \to \gamma\gamma$ and normalizing those of the decays that lead to DVCS contamination by the number of decays leading to a detected π^0. The number of decays was optimized between desired statistics and processing time. In the simulation, pair conversion for the photons and calorimeter reconstruction efficiency were both taken into account. Figure 2 shows the integrated distributions of two exclusivity variables, the squared missing mass and the

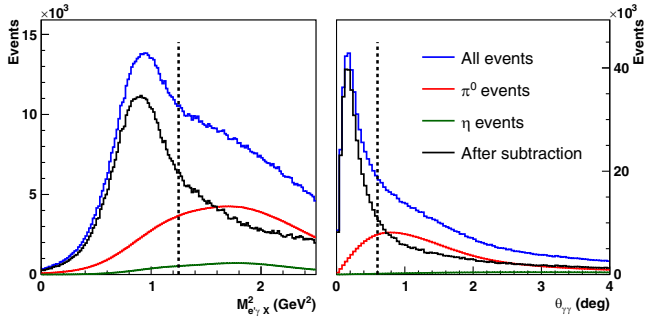

FIG. 2. Squared missing mass $M^2_{e'\gamma X}$ (left) and cone angle $\theta_{\gamma\gamma}$ (right) distributions prior to the application of any exclusivity cuts, for the full dataset showing the π^0 and η contamination and after subtraction. Dashed lines indicate the position of the cuts.

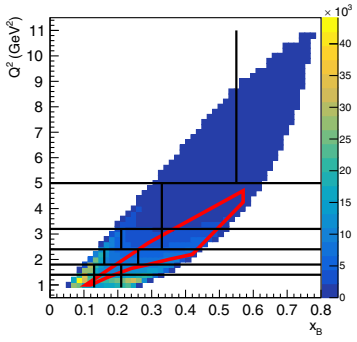

FIG. 3. CLAS12 phase space in Q^2 vs x_B, showing the division into 16 bins. The red line indicates the data coverage of CLAS at 6 GeV.

cone angle, for the determined π^0 contamination, the negligible contribution of η production (estimated with the same method), and the DVCS-BH sample after meson-background subtraction.

The π^0 contamination was determined for each helicity state, thus entangling the π^0 beam-spin asymmetry in the subtraction from the distributions passing the DVCS selection, which was done on a bin-by-bin basis. In addition to the statistical uncertainty induced by the subtraction of the π^0 events, the systematic uncertainty related to it is given for each bin by

$$\Delta A = \frac{\sigma_f \times (A^{\text{raw}} - A^{\pi})}{(1-f)^2}, \tag{2}$$

where f is the fraction of contamination, σ_f is the associated uncertainty, and A^{raw} and A^{π} are the asymmetries prior to π^0 contamination subtraction and of the subtracted π^0 contamination, respectively. Using Monte Carlo simulations with two different π^0 event generators (DVCSGEN [32,33] and AAO_RAD [34]), we estimated $\sigma_f = 0.1 \times f$. As the π^0 statistics may not be high enough to derive its beam-spin asymmetry with accuracy, A^{π} was set to 0 for a conservative estimate of the systematics. Since the fraction of contamination depends on exclusivity cuts as well as on the ratio between the DVCS and π^0 cross sections, and thus varies from bin to bin, the systematic uncertainty was added quadratically to the statistical uncertainty of the DVCS beam-spin asymmetry.

The detection of the scattered lepton in $ep \to e'p'\gamma$ allows one to describe the reaction kinematics in terms of the variables $Q^2 = -q^2 = -(k-k')^2$ and $x_B = Q^2/(2qN)$ (see Fig. 1). The variables t and ϕ (the angle between the leptonic and hadronic planes in the process) were computed using the scattered lepton kinematics and the direction of the photon, the latter being a well-reconstructed quantity. As shown in Fig. 3, there are 16 bins covering the Q^2/x_B phase space. Each Q^2/x_B bin was further subdivided into 4 bins in $t_{\min}(Q^2, x_B) - t$, with $t_{\min}(Q^2, x_B)$ the minimal squared momentum transfer. An adaptive binning was implemented for the variable ϕ, as the cross section exhibits a steep dependence on this variable. The widths of the ϕ bins were allowed to vary, chosen to optimize the statistics in each bin, while, on the one hand, remaining above the ϕ resolution and, on the other hand, keeping the bins sufficiently narrow to minimize acceptance effects. For each $Q^2/x_B/t/\phi$ bin, the averaged kinematic values were computed, corrected for the π^0 contamination bias. Detector acceptance and fiducial cuts applied for particle selection result in a non-negligible variation of x_B and t, which can be observed as a function of ϕ. Thus, the average kinematics are not necessarily the same for neighboring ϕ bins.

Radiative effects, where either a soft photon was radiated by the incoming or outgoing electron, or there was a QED loop involving the virtual photon vertex, were considered and corrected for. These effects may result in bin migration—where the reconstructed kinematics of an event differ from the true kinematics at the vertex. The bin migration was corrected by deriving a migration matrix from a Monte Carlo simulation using a DVCS event generator that included soft photon radiation, based on the calculations by Akushevich and Ilyichev [33].

Results.—In total, the beam-spin asymmetry was obtained for 64 bins in Q^2, x_B, and t, each of which contained between 10 and 33 bins in ϕ, separately for the two datasets obtained with a beam energy of 10.2 and 10.6 GeV. These datasets provide a tremendous addition to the world data. In order to put the results of the CLAS12 datasets into perspective, we will refer to two studies performing global fits, prior to the inclusion of the current data, using very different approaches. The first study has been performed by Kumericki *et al.* and is based on a GPD-hybrid model [35], with sea partons described by a Mellin-Barnes partial-wave expansion, while dispersion relation techniques are applied to the valence region. The few parameters of the model are then fitted against most of the DVCS data available, yielding the KM15 model. The second approach, developed by the PARTONS

Collaboration, is based on artificial neural networks (ANNs) [36,37], trained on the world dataset of DVCS measurements. In both the KM15 and ANN methods, the fit in the valence region occurs at the level of Compton form factors. As is the case for any neural-network-based approach, the ANN method leads to a minimally biased description of the DVCS measurements. To propagate uncertainties, the PARTONS Collaboration smeared the datasets 100 times according to the quoted systematic uncertainties by the experimental collaborations, thus yielding a library of 100 ANNs whose mean is the fitted CFF value and whose standard deviation provides the CFF uncertainty.

For bins in phase space that are sufficiently close to or partly overlapping with the ANN training measurements, it is possible to use a Bayesian reweighting technique to test each ANN against the DVCS asymmetries presented in this Letter. Regularly applied in the parton distribution function field [38], the technique consists of computing a weight associated with each ANN, which reflects how closely it agrees with the new data. The weight ω_k associated with the k replica is given by [39]

$$\omega_k = \frac{1}{Z}\chi_k^{n-1} e^{-(\chi_k^2/2)}, \tag{3}$$

where $Z = \sum_k \chi_k^{n-1} e^{-(\chi_k^2/2)}$, n is the number of points used to compute $\chi_k^2 = \sum_n (y - y_n) V^{-1} (y - y_n)^T$, y are the asymmetry values from CLAS12 with V as the associated covariance matrix, and y_n are the predictions of the k replica. By computing the weighted average and standard deviation of the 100 ANNs, the impact of the CLAS12 data can thus be visualized. As outputs of a minimally biased approach, the ANN fits provide a firm constraint on CFFs only within the training phase space. Therefore, to perform the reweighting, two $Q^2/x_B/t$ bins that had similar kinematics to previously published CLAS data were chosen. In Fig. 4, it can be seen that both KM15 and ANN predictions agree very well, but seem to slightly underestimate the asymmetry at $x_B = 0.15$. Although in similar kinematics to previous CLAS data, this new dataset obtained using a significantly different beam energy provides measurements of beam-spin asymmetry, presented in this Letter, as well as of an unpolarized cross section which will be extracted in a near future. These two observables may thus bring new constraints to separate the imaginary and real parts of CFFs through a Rosenbluth separation.

The quantity N_{eff} allows one to estimate an effective number of ANNs contributing significantly to the reweighted average and standard deviation,

$$N_{\text{eff}} = \exp\left(-\sum_{k=1}^{N_{\text{rep}}} \omega_k \ln \omega_k\right). \tag{4}$$

N_{eff} is found to be ~30 in Fig. 4, meaning that the precision of the new data provided by CLAS12 rejects 70% of the

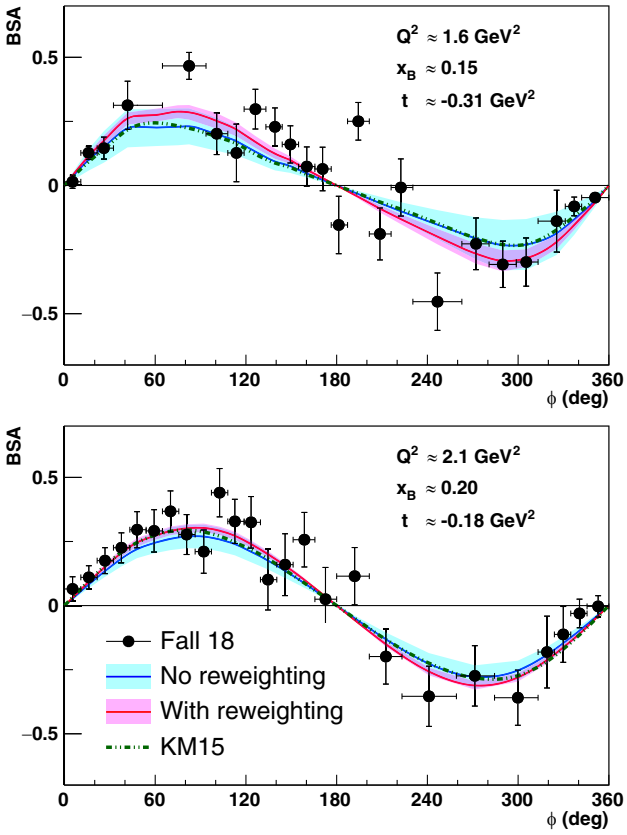

FIG. 4. Beam-spin asymmetries in two kinematic bins, compared with PARTONS ANNs before and after reweighting, as well as with KM15. The kinematics listed are approximate; point-by-point kinematics are available in the tables of the Supplemental Material [40].

ANNs that are in agreement with the Jefferson Lab 6 GeV data within the statistical accuracy. Its constraining and highly discriminative power illuminates the necessity for a full global fit of all world data sensitive to CFFs, with the inclusion of this vast, newly collected dataset.

Figure 5 displays three additional bins in regions of phase space that could only be reached with a 10 GeV beam. Established GPD models, such as Goloskokov-Kroll (GK) [41,42] and Vanderhaeghen-Guichon-Guidal (VGG) [43,44], describe the new data in the unexplored phase space reasonably well, while KM15 seems to underestimate the amplitude of the asymmetry for some of the new bins.

Conclusion.—In conclusion, we report the first measurements of the beam-spin asymmetry in deeply virtual Compton scattering with a lepton beam energy of just over 10 GeV. This has extended the explored Q^2 and x_B phase space greatly beyond the valence-region measurements done at Jefferson Lab with a 6 GeV beam. Together with future measurements of unpolarized cross sections from the same dataset, the new beam-spin asymmetry (BSA) measurements will allow results from both 6 and 10 GeV beam energies to be studied in a Rosenbluth-like

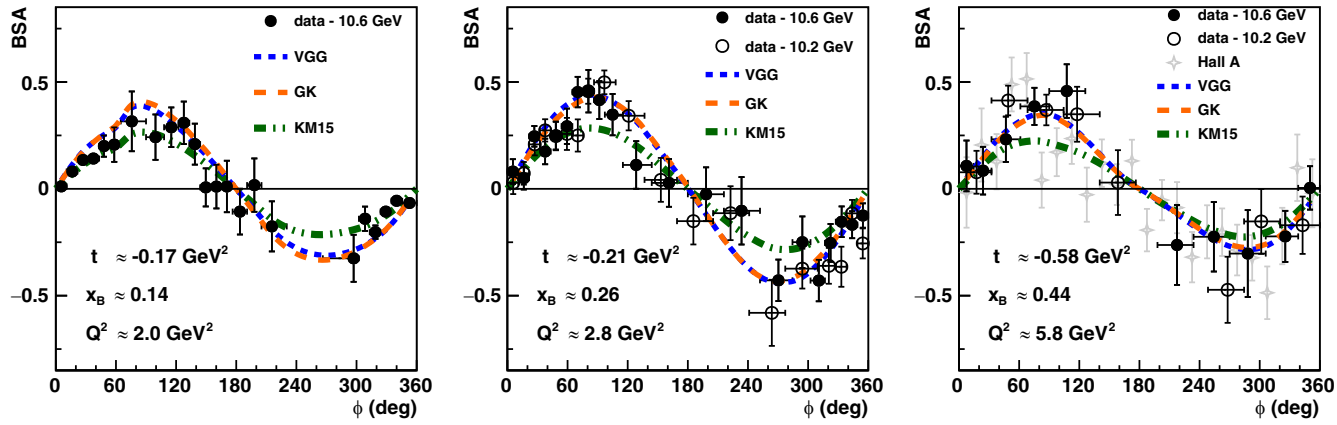

FIG. 5. Beam-spin asymmetries for bins only reachable with a ∼10 GeV electron beam, compared with the KM15, GK, and VGG GPD models. The kinematics listed are approximate; point-by-point kinematics are available in the tables of the Supplemental Material for the full dataset [40]. In the last bin, Hall A asymmetries have been computed from the data published in [22] at $Q^2 = 5.36$ GeV^2, $x_B = 0.48$, and $t = -0.51$ GeV^2.

separation to access the purely DVCS terms in the scattering amplitude.

Although representing only 25% of the beam time allocated to the CLAS12 experiment for DVCS on an unpolarized proton, these new results are already statistically competitive with the entire 6 GeV program, as demonstrated by the reweighting technique. In the *terra incognita*, which forms the great majority of the phase space covered by the new measurement and accounts for almost 89% of the points, while GPD models seem to be in fair agreement with the newly collected data, some tension can be seen with the KM15 global fit. This illuminates the need for the inclusion of the new data, which have greatly enriched the world set, extending the probed phase space in the valence region with high-precision measurements, and promise to provide both very significant constraints for global fits across new kinematic ranges and a crucial means of validating and refining GPD models. All data points can be found in the Supplemental Material [40].

We acknowledge the outstanding efforts of the staff of the Accelerator, the Nuclear Physics Division, Hall B, and the Detector Support Group at JLab that have contributed to the design, construction, installation, and operation of the CLAS12 detector. We thank Maurizio Ungaro for his contributions in the CLAS12 simulations. We also thank the CLAS Collaboration for staffing shifts and taking high quality data. This work was supported by the U.S. Department of Energy under JSA/DOE Award No. DE-AC05-06OR23177. This work was also supported in part by the U.S. National Science Foundation, State Committee of Science of the Republic of Armenia, Chilean Agencia Nacional de Investigación y Desarrollo, Italian Istituto Nazionale di Fisica Nucleare, French Centre National de la Recherche Scientifique, French Commissariat a l'Energie Atomique, Scottish Universities Physics Alliance (SUPA), United Kingdom Science and Technology Facilities Council (STFC), National Research Foundation of Korea, and Deutsche Forschungsgemeinschaft (DFG). This research was funded in part by the French Agence Nationale de la Recherche Contract No. 37. This work was supported as well by the EU Horizon 2020 Research and Innovation Program under the Marie Sklodowska-Curie Grant Agreement No. 101003460 and the Ile-de-France region via the Blaise Pascal Chair of International Excellence. This work has been funded by the U.K. Science and Technology Facilities Council under Grants No. ST/P004458/1 and No. ST/V00106X/1 and in part by the Chilean National Agency of Research and Development ANID PIA/APOYO AFB180002.

*Corresponding author.
maxime.defurne@cea.fr
†Present address: Argonne National Laboratory, Argonne, Illinois 60439, USA.

[1] D. Müller, D. Robaschik, B. Geyer, F.-M. Dittes, and J. Hořejši, Fortschr. Phys. **42**, 101 (1994).
[2] A. Radyushkin, Phys. Lett. B **380**, 417 (1996).
[3] X. Ji, Phys. Rev. D **55**, 7114 (1997).
[4] M. Burkardt, Phys. Rev. D **62**, 071503(R) (2000).
[5] M. Polyakov, Phys. Lett. B **555**, 57 (2003).
[6] A. V. Belitsky, D. Mueller, and A. Kirchner, Nucl. Phys. **B629**, 323 (2002).
[7] P. Kroll, H. Moutarde, and F. Sabatie, Eur. Phys. J. C **73**, 2278 (2013).
[8] C. Adloff *et al.* (H1 Collaboration), Phys. Lett. B **517**, 47 (2001).
[9] H1 Collaboration, Eur. Phys. J. C **44**, 1 (2005).
[10] F. Aaron *et al.* (H1 Collaboration), Phys. Lett. B **659**, 796 (2008).
[11] F. Aaron *et al.* (H1 Collaboration), Phys. Lett. B **681**, 391 (2009).
[12] S. Chekanov *et al.* (ZEUS Collaboration), Phys. Lett. B **573**, 46 (2003).

[13] ZEUS Collaboration, J. High Energy Phys. 05 (2009) 108.
[14] A. Airapetian *et al.* (HERMES Collaboration), J. High Energy Phys. 07 (2012) 032.
[15] R. Akhunzyanov *et al.* (COMPASS Collaboration), Phys. Lett. B **793**, 188 (2019); **800**, 135129(E) (2020).
[16] P. Joerg (COMPASS Collaboration), Proc. Sci. DIS2016 (**2016**) 235 [arXiv:1702.06315].
[17] C. Muñoz Camacho *et al.* (Jefferson Lab Hall A, Hall A DVCS Collaborations), Phys. Rev. Lett. **97**, 262002 (2006).
[18] M. Defurne *et al.* (Jefferson Lab Hall A Collaboration), Phys. Rev. C **92**, 055202 (2015).
[19] M. Defurne *et al.* (Jefferson Lab Hall A Collaboration), Nat. Commun. **8**, 1408 (2017).
[20] M. Mazouz *et al.* (Jefferson Lab Hall A Collaboration), Phys. Rev. Lett. **99**, 242501 (2007).
[21] M. Benali *et al.* (Jefferson Lab Hall A Collaboration), Nat. Phys. **16**, 191 (2021).
[22] F. Georges *et al.* (Jefferson Lab Hall A Collaboration), Phys. Rev. Lett. **128**, 252002 (2022).
[23] S. Stepanyan, V. D. Burkert, L. Elouadrhiri *et al.* (CLAS Collaboration), Phys. Rev. Lett. **87**, 182002 (2001).
[24] S. Chen *et al.* (CLAS Collaboration), Phys. Rev. Lett. **97**, 072002 (2006).
[25] F. X. Girod *et al.* (CLAS Collaboration), Phys. Rev. Lett. **100**, 162002 (2008).
[26] H. S. Jo *et al.* (CLAS Collaboration), Phys. Rev. Lett. **115**, 212003 (2015).
[27] E. Seder *et al.* (CLAS Collaboration), Phys. Rev. Lett. **114**, 032001 (2015).
[28] S. Pisano *et al.* (CLAS Collaboration), Phys. Rev. D **91**, 052014 (2015).
[29] N. Hirlinger Saylor *et al.* (CLAS Collaboration), Phys. Rev. C **98**, 045203 (2018).
[30] V. Burkert *et al.*, Nucl. Instrum. Methods Phys. Res., Sect. A **959**, 163419 (2020).
[31] R. De Masi *et al.* (CLAS Collaboration), Phys. Rev. C **77**, 042201 (2008).
[32] V. A. Korotkov and W. D. Nowak, Eur. Phys. J. C **23**, 455 (2002).
[33] I. Akushevich and A. Ilyichev, Phys. Rev. D **98**, 013005 (2018).
[34] A. Kim and V. Kubarovsky, The AAO_RAD generator, available at https://github.com/JeffersonLab/aao-gen.
[35] K. Kumericki and D. Müller, EPJ Web Conf. **112**, 01012 (2016).
[36] B. Berthou *et al.*, Eur. Phys. J. C **78**, 478 (2018).
[37] H. Moutarde, P. Sznajder, and J. Wagner, Eur. Phys. J. C **79**, 614 (2019).
[38] W. T. Giele and S. Keller, Phys. Rev. D **58**, 094023 (1998).
[39] H. Dutrieux, V. Bertone, H. Moutarde, and P. Sznajder, Eur. Phys. J. A **57**, 250 (2021).
[40] See Supplemental Material at http://link.aps.org/supplemental/10.1103/PhysRevLett.130.211902 for all DVCS BSA measurements.
[41] S. V. Goloskokov and P. Kroll, Eur. Phys. J. C **42**, 281 (2005).
[42] S. V. Goloskokov and P. Kroll, Eur. Phys. J. C **65**, 137 (2009).
[43] M. Guidal, M. V. Polyakov, A. V. Radyushkin, and M. Vanderhaeghen, Phys. Rev. D **72**, 054013 (2005).
[44] M. Guidal, H. Moutarde, and M. Vanderhaeghen, Rep. Prog. Phys. **76**, 066202 (2013).